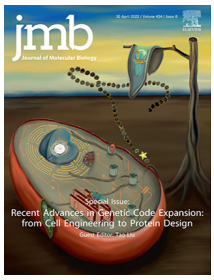

Development of Monoclonal Antibodies to Detect for SARS-CoV-2 Proteins

Nawneet Mishra [1†], Joan Teyra [2†], RuthMabel Boytz [3], Shane Miersch [2], Trudy N. Merritt [4], Lia Cardarelli [2], Maryna Gorelik [2], Filip Mihalic [5], Per Jemth [5], Robert A. Davey [3], Sachdev S. Sidhu [2*], Daisy W. Leung [4*] and Gaya K. Amarasinghe [1*]

*1 - **Department of Pathology and Immunology,** Washington University School of Medicine in St Louis, St Louis, MO 63110, USA*
*2 - **The Donnelly Centre,** University of Toronto, Toronto, Canada*
*3 - **Department of Microbiology,** Boston University School of Medicine, Boston, MA 02118, USA*
*4 - **Department of Medicine,** Washington University School of Medicine, St Louis, MO 63110, USA*
*5 - **Department of Medical Biochemistry and Microbiology,** Uppsala University, BMC Box 582, Husargatan 3, 751 23 Uppsala, Sweden*

***Correspondence to Sachdev S. Sidhu, Daisy W. Leung and Gaya K. Amarasinghe:** gamarasinghe@wustl.edu (G.K. Amarasinghe)*
https://doi.org/10.1016/j.jmb.2022.167583
Edited by Igor Stagljar

Abstract

The COVID-19 pandemic caused by SARS-CoV-2 infection has impacted the world economy and health-care infrastructure. Key reagents with high specificity to SARS-CoV-2 proteins are currently lacking, which limits our ability to understand the pathophysiology of SARS-CoV-2 infections. To address this need, we initiated a series of studies to generate and develop highly specific antibodies against proteins from SARS-CoV-2 using an antibody engineering platform. These efforts resulted in 18 monoclonal antibodies against nine SARS-CoV-2 proteins. Here we report the characterization of several antibodies, including those that recognize Nsp1, Nsp8, Nsp12, and Orf3b viral proteins. Our validation studies included evaluation for use of antibodies in ELISA, western blots, and immunofluorescence assays (IFA). We expect that availability of these antibodies will enhance our ability to further characterize host-viral interactions, including specific roles played by viral proteins during infection, to acquire a better understanding of the pathophysiology of SARS-CoV-2 infections.

Introduction

The SARS-CoV-2 pandemic that began in 2019 highlights the urgent need for the rapid development of reagents to better understand viral pathogenesis, host responses, and to develop diagnostics. SARS-CoV-2 is a positive-sense, single-stranded RNA virus with a genome of approximately 30 kb. Two-thirds of the 5′ end of the viral genome encodes for Non-structural proteins (Nsp) as a polyprotein, which self-cleaves by viral proteases and contributes to virus replication.[1] For example, Nsp1 has a role in translational shutdown and evasion of host immune response,[2] and Nsp12 is the RNA-dependent RNA polymerase, which is essential for virus replication.[3] The last one-third of the genome encodes for the structural envelope (E), membrane (M), and nucleocapsid (N) proteins, in addition to the non-essential accessory proteins. Among them, N

and S proteins have been the major focus for the development of effective therapeutics based on monoclonal antibodies (mAbs) that would neutralize viral infection.[4] While a range of immune sera-derived polyclonal antibodies (pAbs) are available against SARS-CoV-2, there are few mAbs available against non-spike SARS-CoV-2 proteins (Table S1). Polyclonal antibodies (pAbs) are heterogeneous mixtures of antibodies (Abs) that can recognize and bind to many different epitopes of a single antigen, but batch-to-batch inconsistency can complicate reproducibility, and the undefined nature of their many epitopes limits their use in detailed molecular characterization. In contrast, mAbs typically recognize only a single epitope and are an indispensable resource in the fields of immunology, biotechnology, biochemistry, and applied biology due to their homogeneity, specificity, and renewability.[5] The lack of mAbs for SARS-CoV-2 viral proteins constitute a major bottleneck in evaluating cellular responses to vaccines and therapeutics.[6–9] Therefore, efforts towards the generation of mAb reagents targeting as many of the SARS-CoV-2 viral proteins are necessary.

Here, we report the generation, characterization, and optimization of Abs targeting nine different SARS-CoV-2 proteins, including structural, non-structural, and accessory proteins. For this, we expressed and purified 21 recombinant SARS-CoV-2 proteins, carried out Ab selections by phage display, and validated binding of the IgGs to their cognate target *in vitro*. Due to their critical function in multiple steps of viral pathogenesis and infection cycle, 18 mAbs against Nsp1, Nsp8, Nsp12 and Orf3b were further characterized for activity in western blot (WB) and immunofluorescence (IF) assays with SARS-CoV-2-infected cells. Overall, our data provides a strong foundation for using these synthetic Abs to study different SARS-CoV-2 viral proteins and for the development of novel diagnostic assays for COVID-19.

Methods

Protein expression and purification

SARS-CoV-2 proteins were expressed as glutathione S-transferase (GST) or maltose binding protein (MBP) fusion proteins in BL21 (DE3) *Escherichia coli* cells (Novagen). Protein expression was induced at an OD_{600nm} of 0.6 with 0.5 mM isopropyl-β-thiogalactopyranoside for 12–15 h at 18 °C. Cells were harvested, resuspended in lysis buffer containing 25 mM Tris (pH 7.5), 150 mM NaCl, 20 mM imidazole, and 5 mM 2-mercaptoethanol, lysed using an EmulsiFlex-C5 homogenizer (Avestin) and clarified by centrifugation at 30,000*g* at 4 °C for 40 min. MBP-fused proteins were purified using an MBPTrap HP column (GE Healthcare) and ion exchange chromatography. GST-fused proteins were purified using glutathione sepharose 4 Fast Flow media (GE Healthcare) according to the manufacturer's protocols and eluted in buffer containing 50 mM Tris pH 7.8, 300 mM NaCl, 5 mM DTT.

Selection and characterization of Fabs

Fab-phage clones specific for the SARS-CoV-2 proteins (Table S2) were isolated from phage-displayed antibody libraries[10] by four consecutive rounds of binding selections with the SARS-CoV-2 proteins immobilized in microwell plates, as described.[10] Individual colonies were isolated from *E. coli* infected with phage outputs from rounds 3 and 4, and about 48 Fab-phage clones were amplified per antigen. Antibody variable domains of the clones that bound to antigen in Fab-phage ELISA were sequenced by PCR amplification, and unique clones were selected.

To estimate affinities of individual antigen binding clones, a two-point competitive phage ELISA was performed as described.[11] Phage supernatants were diluted in PBT buffer and incubated with either 250 nM or 50 nM antigen in solution for 1-hour. The mixtures were transferred to antigen-coated plates and incubated for 15 min. The plates were washed, incubated 30 min with horseradish peroxidase/anti-M13 antibody conjugate (1:5000 dilution in PBT buffer), developed with TMB substrate (KPL Labs, Gaithersburg, MD), and quenched with 0.5 M H_2SO_4 before measuring absorbance at 450 nm. The fraction of Fab-phage not bound to solution-phase antigen was determined as the ratio of phage captured in the presence and absence of solution-phase antigen (Figure 1(B)). Fab-phage clones presenting the lowest signal ratio were converted to an IgG format for further characterization (Figure 2(A)).

Expression and purification of IgG proteins

Phage clone variable domain DNA was amplified by PCR and subcloned into pSCSTa-hIg1 and pSCST1-hk vectors. Vectors for the heavy and light chains were transfected into HEK293F cells (Invitrogen, Grand Island, NY) using FectoPro according to the manufacturer's instructions (Polyplus Transfection, NY). Cell cultures were incubated at 37 °C for 4–5 days post-transfection. The cell cultures were centrifuged, and the supernatants were applied to a protein-A affinity column (~2 mL packed beads per 600 mL culture) (Pierce, ThermoScientific, Rockford, IL). IgG proteins were eluted with 100 mM glycine, pH 2.0 and neutralized with 2 M Tris, pH 7.5. The eluent underwent buffer exchange on PBS, pH 7.4, and concentrated by centrifugation in a 50 kDa concentrator (Millipore ACS505024).

IgG binding ELISAs

For binding ELISA experiments, 384-well microplates were coated overnight at 4 °C with 2 μg/mL protein or GST/MHT control proteins in PBS pH 7.4. After coating, wells were blocked with 0.2% BSA in PBS for one hour and washed 4 times with 0.05% Tween in PBS (PT buffer). Serial dilutions of IgG diluted into PBT were transferred to antigen-coated plates and incubated at room temperature for 30 min, washed with PBST four times and incubated for 30 min with anti-k-HRP antibody conjugate (1:7500 dilution in PBT), which were washed, developed, and read, as described above. To estimate EC_{50} values, data were fit to standard four-parameter logistic equations using GraphPad Prism (GraphPad Software, La Jolla, CA).

Binding kinetics

To determine binding kinetic parameters of IgGs for SARS-CoV2 proteins, BLI experiments were performed on an Octet HTX instrument (Sartorius) at 1000 rpm and 25 °C. All proteins were diluted in PBS containing 1% BSA and 0.05% Tween 20. 2–20 μg/mL of SARS-CoV2 antigens or unrelated protein with similar size were first covalently captured on AR2G biosensors (Sartorius, 18-5092) by amine-reactive coupling chemistry, and unbound reactive *N*-hydroxysulfosuccinimide (NHS) esters on the biosensors were quenched for 600 s by 1 M ethanolamine (pH 8.5). After equilibrating with assay buffer, the antigen-coated sensors were dipped for 600 s into wells containing serial 3-fold dilutions of IgGs and subsequently were transferred back into assay buffer for 600 s of dissociation. Binding response data were reference subtracted and were globally fitted with 1:1 binding model using ForteBio's Data Analysis software 9.0.

Western blot analyses

Purified protein (0.3 μg) was run on SDS-PAGE gels including a Precision Plus Protein Dual Color Standard (Bio-Rad) for size determination and transferred onto 0.22 μm PVDF membranes (Bio-Rad) in buffer containing 20% methanol, 25 mM Tris HCl, 193 mM glycine) at 4 °C for 2 h. Membranes were blocked in PBS containing 5% skim milk for 60 min. Primary antibody incubation (1:1000) was performed in blocking solution at 25 °C for 2 h and washed thoroughly prior to incubation with secondary antibody (1:5000, rabbit anti-mouse IgG HRP conjugated; Cruz Biotechnologies) for 1 h at 25 °C. Membranes were developed and imaged using a ChemiDoc MP gel imaging system (GE).

Immunofluorescence staining

VeroE6 cells obtained from ATCC (Manassas, VA, USA) were grown in DMEM supplemented with 10% FBS. SARS-CoV-2 isolate USA-WA1/2020 was obtained from BEI Resources (Manassas, VA, USA) and passaged several times on VeroE6 cells to obtain a working virus stock. Cells were seeded into 8-well μ-Slides (Ibidi 80826), allowed to settle overnight, and then infected with SARS-CoV-2 at an MOI of ~0.2 for 24 h. Following infection, cells were fixed in 10% formalin overnight. Cells were washed in PBS, permeabilized in 0.1% Triton X-100 for 15 min and blocked in 5% v/v normal goat serum (GeminiBio 100–109) in PBS for 1 h. Cells were then labelled with one of the following primary antibodies overnight at 4 °C in NGS: anti-Orf3b 15887 (1:2000); anti-Nsp12 15884 (1:3000); anti-Nsp8 15525 and 15524 (1:1000); anti-Nsp1 15498 (1:1500); or 15497 anti-Nsp1 (1:1000). Secondary labelling was performed with a goat anti-human antibody conjugated to Alexa Fluor488 (Invitrogen A11013) at 1:1000 for 2 h at RT, washed in PBS, and stained with Hoechst 33342 (Invitrogen H3570). Cells were subsequently immunolabelled as above with a primary rabbit antibody against SARS-CoV-2 N protein (Sino Biological 40143-R004) at 1:20000 and a goat anti-rabbit secondary antibody conjugated to Alexa Fluor546 (Invitrogen A11035) at 1:1000. Cells were imaged using a Nikon Ti-2 Eclipse fluorescence wide field microscope fitted with a scientific CMOS camera (Prime-BSI, Photometrics) and LED light source.

Results

Using a phage-displayed human antigen-binding fragment (Fab) library, library F (Persson et al., 2013), we performed four rounds of selection for binding to 18 SARS-CoV-2 proteins (Figure 1, Table S2). For each antigen, 48 Fab-phage clones from selection outputs were screened by ELISA to compare binding to the cognate immobilized SARS-CoV-2 protein along with several negative control proteins (maltose binding protein (MBP), glutathione S-transferase (GST), and native bovine serum albumin (BSA), Figure 1(B)). Unique Fab clones that bound specifically to corresponding SARS-CoV-2 proteins were identified by DNA sequencing of the complementarity-determining regions (CDRs) from the variable chains.

To prioritize our efforts on clones that bound more tightly to the target, we carried out a two-point competitive ELISA,[11] in which positive Fab-phage clones were pre-incubated with their cognate soluble antigen. Uncomplexed Fab-phage were then captured by immobilized antigen and the phage-binding signal compared to the phage-binding signal in the absence of soluble antigen (Figure 1 (B)). Smaller ratios are indicative of higher affinity

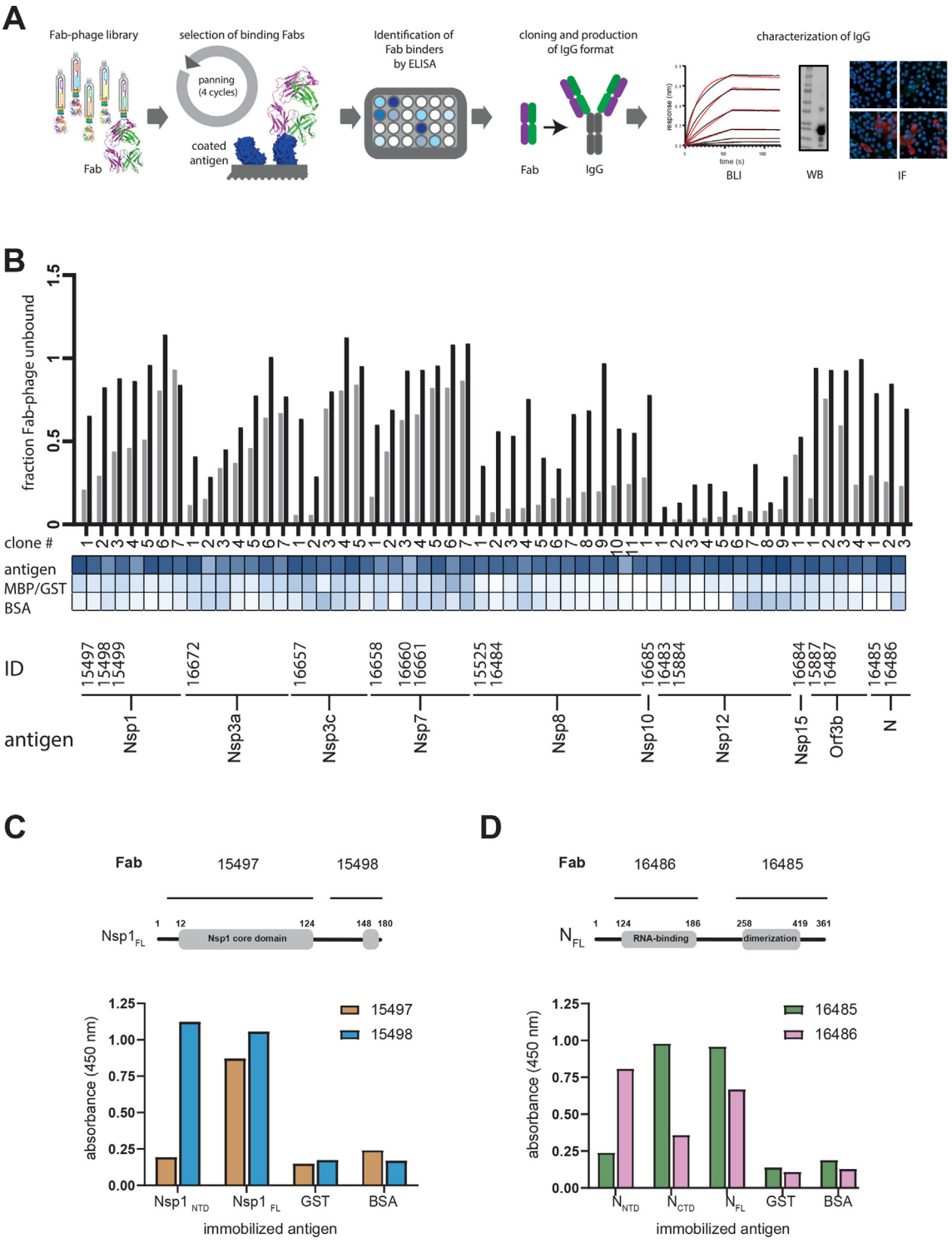
A
Fab-phage library
selection of binding Fabs
panning (4 cycles)
coated antigen
Identification of Fab binders by ELISA
cloning and production of IgG format
Fab
IgG
characterization of IgG
BLI
WB
IF
B
fraction Fab-phage unbound
clone #
antigen
MBP/GST
BSA
ID
antigen
Nsp1
Nsp3a
Nsp3c
Nsp7
Nsp8
Nsp10
Nsp12
Nsp15
Orf3b
N
C
Fab
15497
15498
Nsp1FL
Nsp1 core domain
absorbance (450 nm)
Nsp1 NTD
Nsp1 FL
GST
BSA
immobilized antigen
D
Fab
16486
16485
NFL
RNA-binding
dimerization
NNTD
NCTD
NFL
GST
BSA
immobilized antigen

due to increased Fab-phage binding to solution-phase antigen, and consequently, less captured by the immobilized antigen. For each SARS-CoV-2 protein, clones that exhibited the lowest binding ratios in the two-point competitive assay (indicating tight binding to soluble protein) were selected for further characterization (Figure 1(B)). In addition, to obtain clones targeting distinct SARS-CoV-2 epitopes on the same protein, selections were carried out against five domains of Nsp3, including domains 3a, 3b, 3c, 3d and 3e (Table S2). This resulted in the isolation of Fab-phage clones that bound specifically to epitopes located in domains 3a and 3c (Table S2). For Nsp1 and N proteins, selections were carried out against the full-length (FL) proteins, and isolated Fab-phage clones were then evaluated against the FL, N-terminal (NTD) and C-terminal (CTD) domains by ELISA enabling identification of Fab-phage clones binding the NTD and CTD epitopes of both proteins (Figure 1(C and D), respectively). Together, the competitive assay and the epitope mapping results obtained with Fab-phages were used to prioritize a total of 18 clones that bound to 9 SARS-CoV-2 proteins for sub-cloning, purification and functional characterization of the full-length IgG1 format (Figure 2(A)).

To estimate affinities, ELISAs were performed to assess the binding of serial dilutions of IgGs to immobilized SARS-CoV-2 protein, and revealed that most of the IgGs bound with EC_{50} values in the single-digit nanomolar range Figure 2((A), S1), except for 16485, 16658, and 16684 IgGs, which bound at 19, 130 and 19 nM to N, Nsp7, and Nsp15, respectively. To characterize affinities more quantitatively, binding was also assessed by biolayer interferometry (BLI). For this, purified IgG antibodies were captured on an anti-human Fc capture biosensor (AHC) and the binding kinetics were evaluated with soluble SARS-CoV-2 protein. The majority of the IgGs exhibited sub-nanomolar K_D values, in close accord with the EC_{50} values measured by ELISA Figure 2((A), S1). Unexpectedly, we could not obtain binding signals for 16658 or 16684 IgGs to Nsp7 or Nsp15, respectively, and 15887 IgG bound much more weakly to Orf3b than shown by ELISA. We attribute these problems to the varying immobilization strategies which might differentially present the epitope of the antigen, and in these cases, alter binding.

To further characterize these mAbs, we focused on the IgGs binding to the key viral proteins Nsp1, Nsp8, Nsp12 and Orf3b for their direct involvement into host translation shutdown,[6,21] viral replication[3,12,22], and immune antagonism.[13] We performed western blot (WB) analysis to further evaluate the ability of the mAbs to specifically detect each respective protein. Our results show that these mAbs can be used to detect denatured protein by WB (Figure 2(B–E)). Both Nsp1 mAbs (15497 and 15498) detected a band corresponding to the correct molecular weight of Nsp1 (19.7 kDa) in addition to a lower molecular weight band that likely corresponds to degraded Nsp1 protein. mAbs to Nsp8 (15525) and Nsp12 (15886) showed reactivities to a single band on the blot at the corresponding molecular weight of their antigen (22.6 kDa and 150.6 kDa, respectively). Each of these mAbs showed no reactivity to a negative control maltose binding protein (MBP), thus confirming their specificity.

To assess the suitability of our synthetic Abs in immunofluorescence (IF) assays, VeroE6 cells were grown in 8-well μ-slides and infected with SARS-CoV-2 (MOI 0.2) prior to immunolabeling with expressed IgGs as the primary Ab. A commercially available rabbit Ab to SARS-CoV-2 N protein was used as a control and marker for virus infection.[14,15] When acquiring images for each mAb, we set the laser intensity and exposure such that there was no signal in the 488 channels (channel containing primary antibody) for uninfected cells and maintained these settings when imaging infected cells. Thus, any signal observed in the 488 channel from infected cells is specific binding of the Ab and not a background artifact. mAbs

Figure 1. Synthetic antibody selection and characterization. **(A)** Schematic representation of the strategy in which antibodies were isolated by screening a phage-displayed Fab library for binding to SARS-CoV-2 proteins. Binding clones were identified by ELISA, transformed to IgG format, and characterized *in vitro* and in cells. **(B)** At the top, a plot of the % maximal Fab-phage binding signal in the presence of two different soluble antigen concentrations (gray: 250 nM, black: 50 nM) obtained by a two-point competitive ELISA. Fab-phage clones are ranked from lowest to highest signal ratios. Below the bar graph, Fab-phage clone numbers and binding signals to their cognate antigen obtained by ELISA is compared to negative controls (GST or MHT and BSA) and represented as a heat map with intensities ranging from high (blue) to low (white). At the bottom, the IDs for those antibodies converted to IgGs and their antigens are shown. **(C)** Fab 15497 and 15498 were measured for binding to immobilized Nsp1 N-terminal domain ($Nsp1_{NTD}$), C-terminal domain ($Nsp1_{CTD}$) and full-length protein ($Nsp1_{FL}$). **(D)** Fab 15497 and 15498 were measured for binding to immobilized N N-terminal domain (N_{NTD}), C-terminal domain (N_{CTD}) and full-length protein (N_{FL}). Negative controls (GST, BSA) were also included. Domain organization of Nsp1 and N are included and labeled above each panel in (A) and (B), respectively. Region of respective Fab binding are also indicated.

A

Antigen	ID	ELISA EC_{50} (nM)	BLI K_D (nM)	CDR-L3 107 108 109 110 111 112 113 114 115 116	CDR-H1 30 35 36 37 38 39	CDR-H2 55 56 57 58 59 62 63 64 65 66	CDR-H3 107 108 109 110 111 111.1 111.2 111.3 111.4 111.5 112.5 112.4 112.3 112.2 112.1 112 113 114 115
Nsp1	15497	1.0	0.9	Y Y S - - - - L I	F S S S S I	S I S S S Y G Y T Y	W A - - - - - - - - - - - - - - - A M
Nsp1	15498	0.8	1.4	W Y Y Y - S A A V	I S S S S M	A V A S F Y G A T Y	A Y H - - - - - - - - - - - - - A G L
Nsp1	15499	0.9	0.1	W Y Y Y - S A A V	V A A S S M	A V A A Y Y G S T Y	A Y H - - - - - - - - - - - - - A A L
Nsp3a	16672	2.1	0.1	Y W W - - - Y L F	L S Y Y S M	S I Y P Y Y G S T Y	S P G W W - - - - - - - - - - - G A L
Nsp3c	16657	1.0	1.3	G S Y G A W S L F	L S Y Y Y M	S I S P Y Y G S T S	G W - - - - - - - - - - - - - - - G M
Nsp7	16658	130	*ND*	Y A G - - - - L I	L S Y Y S I	S I Y P Y Y S Y T Y	V - - - - - - - - - - - - - - - - G F
Nsp7	16660	0.5	2.4	S W W V - P F L I	I S Y Y Y I	S I Y S Y Y G Y T Y	S W G G P - - - - - - - - - - G P G I
Nsp7	16661	0.8	2.5	P V W W - P F L I	L S Y S Y I	S I Y P Y Y S Y T Y	A Y Y W Y - - - - - - - - - - S W A M
Nsp8	15525	0.5	1.9	S S Y - - - S L I	F S S S S I	S I S S S Y G Y T Y	S A G W - - - - - - - - - - - - Y A M
Nsp8	16484	0.5	0.2	Y Y P - - F S P I	I Y S S Y M	S I S P S Y G Y T S	P P G P W - - - - - - - - - - G Y A F
Nsp10	16685	0.4	0.6	G W Y - - - - L F	L Y S S Y M	S I Y S S Y G Y T S	H W Y - - - - - - - - - - - - - W G F
Nsp12	16483	2.0	1.8	P Y V - - - G L F	L S Y Y S I	Y I Y P Y Y G Y T S	Y G S Y - - - - - - - - - - - G G M
Nsp12	15884	3.9	12	S H W - - - H P I	I Y Y Y S M	S I Y S Y Y G Y T S	H P A Y - - - - - - - - - - - G G M
Nsp15	16684	19	*ND*	S S Y - - - S L I	F S S S S I	S I Y S S Y G Y T Y	V S Y Y Y P Y S W Y - F Y G Y Y G G L
Orf3b	15887	8.6	261	Y Y H - - Y Y L F	I S Y Y Y M	S I S S Y Y G S T S	W P W Y Y - - - - - - - - - P H G G L
Orf3b	16487	0.8	5.8	G G Y - - W P P F	I S Y Y S M	S I Y P Y Y G Y T S	W W G S G W P G S Y P P G V G H A G L
N	16485	19	20	Y S G Y H F F P I	I Y S S S I	Y I S S Y S G Y T S	V P W Y Y A Y S F - G F F A S F G G M
N	16486	0.8	3.4	S F S - - Y Y P I	I S Y Y Y I	Y I S P Y S G Y T Y	G W S V H - - - - - - - Y P G F H G F

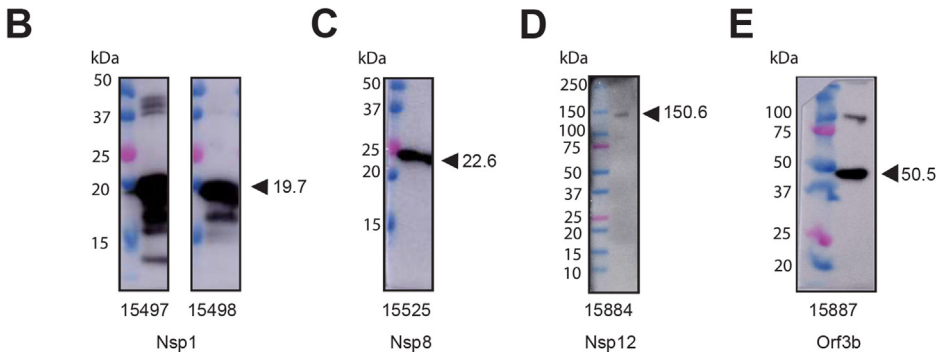

Figure 2. Phage ELISA binding of Fabs sequences and characterization. **(A)** CDR sequences and affinities are shown for the indicated IgGs against their cognate antigen. Sequences are shown for positions that were diversified in the library and are numbered according to IMGT standards,[23] with dashes indicating gaps in the alignment. EC_{50} values were determined by ELISA, whereas dissociation constants (K_D) were determined by BLI (see Figure S1). NB = no binding. **(B–E)** Western blots of Nsp1 (15497 and 15498), Nsp8 (15525), Nsp12 (15884), and Orf3b (15887) antibodies. Colored molecular weight marker is as indicated on the left lane. Protein samples are in the right lane.

against Orf3b (15887), Nsp12 (15884), and Nsp1 (15497) successfully and specifically labeled intracellular viral targets (Figure 3(A)), whereas Nsp1 (15498) did not work for IFA. For each of these Abs, we observed no staining in uninfected cells whereas in cells infected with SARS-CoV-2 we were able to visualize a clear signal above background, indicative of the Abs being specific for each target protein. For the 15497 and 15498 Abs that recognize two different epitopes on Nsp1 Figure 1 ((C)), our results showed a punctate pattern within the nucleus or directly on its edge.[16] We also observed a similar punctate staining for Nsp12 and Orf3b largely in the perinuclear region of infected cells. However, we were unable to visualize targets using the Abs against Nsp8 (15525), which did not result in a detectable stain above background (Figure 3(A)). The fact that IgG binds to Nsp8 *in vitro*, suggests that the IgG epitopes may be inaccessible in the cellular environment. This may be due to the fact that Nsp8 is a small protein (198 amino acids) that functions as a stable heterocomplex with Nsp7 and Nsp12, which is required for replication,[17,18] creating steric hindrance in the IgG recognition in infected cells. Overall, our results validate the use of antibodies 15887, 15884, and to a lesser extent 15497 in IF assays and suitability for characterization of the cellular localization of SARS-CoV-2 viral proteins.

Moreover, sub-cellular localization patterns of Orf3b, and Nsp12 could be visualized by immunofluorescence (IF). In N-stained cells, we found expression of Orf3b in N-expressing cells, but also cells lacking N expression, which suggests that Orf3b is expressed at the early stage of SARS-CoV-2 infection, or it is translocating to neighboring cells (Figure 3(A)). Orf3b exhibited a punctate staining pattern within the cytoplasm of infected cells (Figure 3(B), right panel), which is consistent with previous studies showing SARS-CoV-2 Orf3b localization in the cytosol, where it suppresses IFN-I activation.[13]

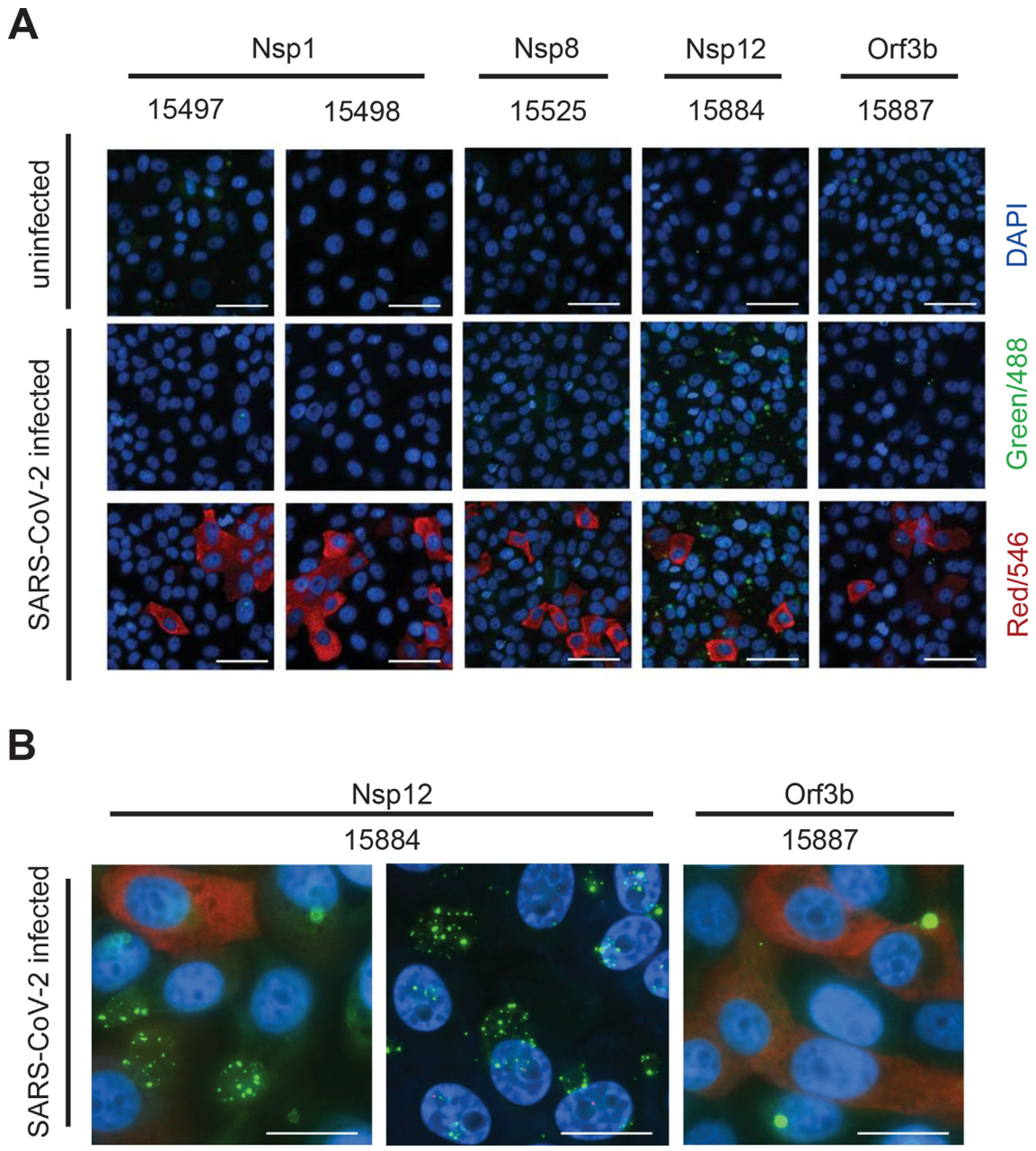

Figure 3. Immunofluorescence staining of SARS-CoV-2 infected VeroE6 cells. **(A)** Panels of uninfected and SARS-CoV-2 infected VeroE6 cells (MOI 0.2) stained with IgGs against Nsp1, Nsp8, Nsp12 or Orf3b (green; λ = 488 nm), nuclei (DAPI, blue), and N (red; λ = 546 nm). Scale bars indicate 50 μm. **(B)** 100$\times$ images of infected VeroE6 cells stained with IgGs against Nsp12 (15884, left and middle panel) or Orf3b (15887, right panel) (green), nuclei (blue), and N (red). Middle panel shows a maximum intensity projection of combined z-planes representing the lower and upper half of the cell bodies stained with Nsp12 of a different frame of the left panel and shown. Scale bars indicate 20 μm.

Unlike Orf3b, Nsp12 appeared as clusters of puncta surrounded by a faint, diffuse background mostly localized to the perinuclear region of infected cells (Figure 3(B), left panel). We noticed that the puncta were distributed across multiple z-planes, which suggests a 3D structure. To better visualize this, we took z-stacks at 100x, followed by image deconvolution, and generated a maximum-intensity projection image (Figure 3(B), middle panel). This structure and localization differ from the cytosolic localization observed by others upon Nsp12 overexpression.[19] In this regard, we observe puncta-like structures or inclusion bodies. Furthermore, N staining shows that N protein is not necessarily highly expressed at the time as the other SARS-CoV-2 proteins and cells with high levels of N staining lacked detectable Nsp12 expression, whereas Nsp12, which is the essential component of the

replication machinery, appears to be detected before an abundance of N protein. Thus, these sites may be indicative of the replication complexes in SARS-CoV-2 infected cells, which are found in both N-expressing and non-expressing cells, like Orf3b (Figure 3(A)). Overall, our results validate the use of antibodies 15884 and 15887 in IF procedures and provide support for their use in studying subcellular locations of SARS-CoV-2 viral proteins. Further optimization will be warranted to fully understand the structures observed here.

Discussion

As the COVID-19 pandemic progresses into the 3rd year, there are many remaining questions surrounding SARS-CoV-2 biology. Here we describe a number of validated critical reagents that provide new tools to better understand viral infection and host responses (Table S1). In this report, we describe our efforts to develop 18 monoclonal IgGs binding specifically to 9 different SARS-CoV2 proteins at sub-nanomolar affinities. We validated and further characterized several mAbs *in vitro*, further demonstrating the potential impact of these reagents. For key targets involved in host response modulation and viral replication, the suitability of these antibodies in WB and IF applications were demonstrated, thus providing validation of the utility of these reagents. IgGs binding to two non-overlapping epitopes for Nsp1, Nsp3 and N proteins were obtained by tailored selections against individual domains. Insofar as pairs of antibodies targeting distinct epitopes have utility in diagnostic and quantitative assays,[20] this basic characterization may help to fast-track applications development or provide tools to evaluate the differential roles of the distinct regions of each of these multi-domain, multi-functional viral proteins. These reagents also have potential utility for a number of assays, such as flow cytometry, immunofluorescence staining, coimmunoprecipitation assays, and for biochemical and structural characterization of the proteins. Our efforts further illustrate the facile implementation of the phage display platform to generate critical reagents to study SARS-CoV-2 proteins and their host interactions leading to a better mechanistic understanding at the host-pathogen interface.

CRediT authorship contribution statement

Nawneet Mishra: Conceptualization, Investigation, Writing – original draft. **Joan Teyra:** Conceptualization, Investigation, Writing – original draft. **Ruthmabel Boytz:** Investigation. **Shane Miersch:** Project administration, Supervision. **Trudy N. Merritt:** Investigation. **Lia Cardarelli:** Investigation. **Maryna Gorelik:** Investigation. **Filip Mihalic:** Investigation. **Per Jemth:** Investigation. **Robert Davey:** Conceptualization, Supervision, Writing – review & editing, Funding acquisition. **Sachdev S. Sidhu:** Conceptualization, Supervision, Writing – review & editing, Funding acquisition. **Daisy W. Leung:** Conceptualization, Supervision, Writing – review & editing, Funding acquisition. **Gaya K. Amarasinghe:** Conceptualization, Supervision, Writing – review & editing, Funding acquisition.

DATA AVAILABILITY

Data will be made available on request.

Acknowledgements

We thank Dr. N. Krogan (UCSF) for sharing SARS-CoV-2 plasmids. We thank Ylva Ivarsson for providing the constructs, which are available at Addgene.

Funding

This work was supported by grants #2161 to GKA and SSS and #2189 to SSS from Emergent Ventures through the Thistledown Foundation (Canada) and the Mercatus Center at George Mason University and NIH grants (P01AI120943, and R01AI161374 to G.K.A.; R01AI140758 to D. W.L.). This study was also supported in part by a CIHR operating grant (COVID-19 Rapid Research Funding #OV3-170649) to SSS.

Declaration of interests

The authors declare that they have no known competing financial interests or personal relationships that could have appeared to influence the work reported in this paper.

Appendix A. Supplementary material

Supplementary data to this article can be found online at https://doi.org/10.1016/j.jmb.2022.167583.

Received 18 February 2022;
Accepted 2 April 2022;
Available online 8 April 2022

Keywords:
SARS-CoV-2;
antibody;
phage display

† Equal contributions.

References

1. Rehman, M.F.U., Fariha, C., Anwar, A., Shahzad, N., Ahmad, M., Mukhtar, S., et al., (2021). Novel coronavirus disease (COVID-19) pandemic: A recent mini review. *Comput. Struct. Biotechnol. J.* **19**, 612–623.
2. Xia, H., Cao, Z., Xie, X., Zhang, X., Chen, J.Y., Wang, H., et al., (2020). Evasion of Type I Interferon by SARS-CoV-2. *Cell Rep.* **33**, 108234.
3. Wilamowski, M., Hammel, M., Leite, W., Zhang, Q., Kim, Y., Weiss, K.L., et al., (2021). Transient and stabilized complexes of Nsp7, Nsp8, and Nsp12 in SARS-CoV-2 replication. *Biophys. J.* **120**, 3152–3165.
4. Thura, M., Sng, J.X.E., Ang, K.H., Li, J., Gupta, A., Hong, J. M., et al., (2021). Targeting intra-viral conserved nucleocapsid (N) proteins as novel vaccines against SARS-CoVs. *Biosci. Rep.* **41**
5. Acharya, P., Quinlan, A., Neumeister, V., (2017). The ABCs of finding a good antibody: How to find a good antibody, validate it, and publish meaningful data. *F1000Research* **6**, 851.
6. Vazquez, C., Swanson, S.E., Negatu, S.G., Dittmar, M., Miller, J., Ramage, H.R., et al., (2021). SARS-CoV-2 viral proteins NSP1 and NSP13 inhibit interferon activation through distinct mechanisms. *PLoS ONE* **16**, e0253089.
7. Brobst, B., Borger, J., (2022). Benefits and risks of administering monoclonal antibody therapy for coronavirus (COVID-19). StatPearls, Treasure Island (FL).
8. Zhang, K., Miorin, L., Makio, T., Dehghan, I., Gao, S., Xie, Y., et al., (2021). Nsp1 protein of SARS-CoV-2 disrupts the mRNA export machinery to inhibit host gene expression. *Sci. Adv.* **7**
9. Prentice, E., McAuliffe, J., Lu, X., Subbarao, K., Denison, M.R., (2004). Identification and characterization of severe acute respiratory syndrome coronavirus replicase proteins. *J. Virol.* **78**, 9977–9986.
10. Persson, H., Ye, W., Wernimont, A., Adams, J.J., Koide, A., Koide, S., et al., (2013). CDR-H3 diversity is not required for antigen recognition by synthetic antibodies. *J. Mol. Biol.* **425**, 803–811.
11. Birtalan, S., Zhang, Y., Fellouse, F.A., Shao, L., Schaefer, G., Sidhu, S.S., (2008). The intrinsic contributions of tyrosine, serine, glycine and arginine to the affinity and specificity of antibodies. *J. Mol. Biol.* **377**, 1518–1528.
12. Chen, J., Malone, B., Llewellyn, E., Grasso, M., Shelton, P. M.M., Olinares, P.D.B., et al., (2020). Structural Basis for Helicase-Polymerase Coupling in the SARS-CoV-2 Replication-Transcription Complex. *Cell* **182** 1560–73 e13.
13. Konno, Y., Kimura, I., Uriu, K., Fukushi, M., Irie, T., Koyanagi, Y., et al., (2020). SARS-CoV-2 ORF3b Is a Potent Interferon Antagonist Whose Activity Is Increased by a Naturally Occurring Elongation Variant. *Cell Rep.* **32**, 108185.
14. Surjit, M., Lal, S.K., (2008). The SARS-CoV nucleocapsid protein: a protein with multifarious activities. *Infect Genet Evol.* **8**, 397–405.
15. Finkel, Y., Mizrahi, O., Nachshon, A., Weingarten-Gabbay, S., Morgenstern, D., Yahalom-Ronen, Y., et al., (2021). The coding capacity of SARS-CoV-2. *Nature* **589**, 125–130.
16. Zhao, K., Ke, Z., Hu, H., Liu, Y., Li, A., Hua, R., et al., (2021). Erratum for Zhao et al., "Structural Basis and Function of the N Terminus of SARS-CoV-2 Nonstructural Protein 1". *Microbiol Spectr.* **9**, e0100221.
17. Kirchdoerfer, R.N., Ward, A.B., (2019). Structure of the SARS-CoV nsp12 polymerase bound to nsp7 and nsp8 co-factors. *Nature Commun.* **10**, 2342.
18. Yan, L., Zhang, Y., Ge, J., Zheng, L., Gao, Y., Wang, T., et al., (2020). Architecture of a SARS-CoV-2 mini replication and transcription complex. *Nature Commun.* **11**, 5874.
19. Wang, W., Zhou, Z., Xiao, X., Tian, Z., Dong, X., Wang, C., et al., (2021). SARS-CoV-2 nsp12 attenuates type I interferon production by inhibiting IRF3 nuclear translocation. *Cell. Mol. Immunol.* **18**, 945–953.
20. Hasegawa, K., Ikeda, S., Yaga, M., Watanabe, K., Urakawa, R., Iehara, A., et al., (2022). Selective targeting of multiple myeloma cells with a monoclonal antibody recognizing the ubiquitous protein CD98 heavy chain. *Sci. Transl. Med.* **14**, eaax7706.
21. Thoms, M., Buschauer, R., Ameismeier, M., Koepke, L., Denk, T., Hirschenberger, M., et al., (2020). Structural basis for translational shutdown and immune evasion by the Nsp1 protein of SARS-CoV-2. *Science* **369**, 1249–1255.
22. Perry, J.K., Appleby, T.C., Bilello, J.P., Feng, J.Y., Schmitz, U., Campbell, E.A., (2021). An atomistic model of the coronavirus replication-transcription complex as a hexamer assembled around nsp15. *J. Biol. Chem.* **297**, 101218.
23. Lefranc, M.P., Pommie, C., Ruiz, M., Giudicelli, V., Foulquier, E., Truong, L., et al., (2003). IMGT unique numbering for immunoglobulin and T cell receptor variable domains and Ig superfamily V-like domains. *Dev. Comp. Immunol.* **27**, 55–77.